

Off-Axis Aberration Correction for a Wide Field Scanning Telescope

Charles Scott[†], Benjamin Potsaid[‡], John T. Wen[†]

[†] Rensselaer Polytechnic Institute, Troy, NY [‡] Thorlabs, Inc., Newton, NJ

ABSTRACT

Due to the tradeoff between field of view and resolution, the ability of traditional optical telescopes to obtain high-resolution wide field images is limited. This work presents a design for a scanning optical telescope that can produce high resolution images over a wide field of view. This is accomplished by scanning one of the telescope's optical elements. Inherent in such a design is the introduction of optical aberrations as off-axis scanning occurs. The deformable mirror technology is implemented to adaptively correct these aberrations such that on-axis resolution is achieved at off-axis scan angles. The optical design layout is optimized in software to minimize on-axis wavefront aberrations. This paper presents results involving two deformable mirrors based on different technologies: the AgilOptics mirror based on electrostatic actuators and the Imagine Optic mirror based on electromagnetic actuators. Both mirrors are similar in size (about 15mm aperture), but the Imagine Optic mirror has significantly larger actuator displacement, though at a higher cost. The static telescope design has a field of view of 0.49-degrees which is increased to 20-degrees with the AgilOptics mirror and 40-degrees with the Imagine Optic mirror.

Keywords: telescope, scanning, wide field of view, deformable mirror, adaptive optics

1. INTRODUCTION

A classical design consideration in the construction of an optical telescope is the tradeoff between field of view and resolution. As the resolution of the system increases, the field of view will decrease. High resolution imaging is desirable for many applications, but a large field of view may also be an important design consideration. Surveillance applications, for example, are not only concerned with high resolution in the immediate field of view, but with the surrounding area as well. This paper will discuss a design concept for a telescope that utilizes adaptive optical elements (scanning mirror and deformable mirror) to overcome classical limitations and produce high resolution images while maintaining a large field of view.

2. RELATED WORK

A traditional approach to expanding the field of view in an optical system is accomplished through a static lens design. A standard wide-angle lens is generally used which involves the use of a strong negatively powered front lens that bends light outward in order to cover a larger field.¹ At very large angles, this bending can give an undesirable "fishbowl" effect where the outer edges of the image become distorted.

A different approach to the same problem is to take many high resolution images at multiple field angles. These images can then be stitched together to form a mosaic of high resolution images with a composite large field of view.² Automatic processes for this method exist, but they involve positioning the object with respect to the image sensor such that all image segments are on the optical axis of the image sensor.³ To keep the image and object on the optical axis, the entire telescope needs to be positioned at a new angle in order to acquire another field. The process of moving the telescope, even if it is automated, is slow due to the large inertia of the entire system. While construction of a high resolution image is possible with this method, it is not capable of producing images fast enough for applications that require rapid image acquisition.

By simply moving one of the optical elements instead of the entire telescope, a high resolution mosaic image can be acquired much faster due to the smaller inertia of a single component. An issue that arises when doing this is that wavefront aberrations are generated when optical elements are moved to positions that are not on-axis with the initial design, resulting in poor image quality. Adaptive optical design recognizes that the performance

of the system will diminish as aberrations increase and provides measures for correcting these aberrations and increasing image quality.

One method of adaptive wavefront aberration correction employed by a wide-field telescope uses a liquid crystal spatial light modulator (SLM) to remove aberrations.⁴ The SLM has addressable pixels that can change their refractive index relative to an applied voltage. As light is reflected at the the SLM, the optical path difference (OPD) of the rays can be altered by adjusting the voltages to the pixels on the array. As the field angle of the telescope is scanned to various positions off-axis, the applied voltages are changed to compensate for the changing aberrations. Other optical designs employ the SLM technology to achieve foveated viewing^{5,6} instead of large field scanning.

A drawback to the SLM technology in these applications is that it is wavelength dependent so it only works with monochromatic light. The OPD using SLM technology is $OPD = n_{pixel} \cdot x$ with n being the index of refraction of the medium and x being the distance traveled through that medium. Due to the wavelength difference of colored light across the visible spectrum, light at a given color will be out of phase with light at a different color over this OPD. Because of this, a design using a SLM requires the incoming light to pass through a filter to transmit only one frequency and the system is optimized to that frequency.^{5,6} This is undesirable as the entire visible spectrum should be able to be viewed.

Deformable mirrors have also been used to correct wavefront aberrations in optical systems. Individual actuators are attached to a mirror and can be controlled to deflect the mirror surface electrostatically or electromagnetically.⁷ These actuators are generally arranged in a grid pattern at varying spatial resolution densities. A microelectromechanical system (MEMS) deformable mirror is a silicon based structure attached to the bottom of a mirror or mirror-membrane surface. Current MEMS based devices are limited as to the amount of deflection they are capable of which is usually on the order of $<10\mu\text{m}$ stroke. Traditionally, deformable mirror technology is used to correct aberrations created outside the optical system such as in astronomical imaging and retina imaging. These systems usually have a wavefront sensor and deformable mirror in a closed-loop control system for real-time aberration detection and compensation.

This paper discusses a scanning telescope design that employs deformable mirror technology for static aberration correction. This design is related to an adaptive scanning optical microscope (ASOM) developed at Rensselaer Polytechnic Institute.⁸ This microscope is designed due to a need for a larger field of view without movement of the specimen being observed. It employs a scanner lens consisting of multiple lens elements through which the specimen is observed. A steering mirror is used to direct the light path over various angles through the scanner lens and a deformable mirror is used to correct any aberrations due to off-axis imaging through the scanner lens. The scanning telescope works in a similar manner by scanning a mirror to observe a larger overall field of view. The desired scanning angle on the telescope is large and associated off-axis aberrations considerable, which requires that the deformable mirror have a large stroke.

3. EXPERIMENTAL DESIGN AND SETUP

ZEMAX is used in the design of the telescope to optimize the rough layout as well as determine aberrations inherent in the design. In order to develop a functional scanning telescope, the wavefront aberrations that are created by scanning to off-axis positions must be within the correctable stroke of the deformable mirror. Simulations are performed in ZEMAX where the tilt of the primary mirror of a Newtonian style telescope is increased to progressively larger off-axis angles and the peak to valley wavefront error is recorded. Results of these simulations are found in Table 1. Here we see the wavefront error (in waves) that must be corrected for by the deformable mirror. For example, at a horizontal tilt of 5-degrees and no vertical tilt, there are 12.8 waves of peak to valley aberration. At a wavelength of 550nm, this corresponds to approximately $7\mu\text{m}$ of optical path difference and requires a mirror stroke of half that ($3.5\mu\text{m}$) in order to fully correct the aberrations. We also see in Table 1 that the peak to valley magnitude of the wavefront increases proportionally to the square of the mirror tilt which is consistent with astigmatism.

The experimental telescope setup is constructed on an optical breadboard with off-the-shelf components and built according to the ZEMAX design (Figure 1). The initial design substitutes a flat mirror in the deformable

Table 1. Simulated Peak-to-Valley Wavefront Error for Horizontal and Vertical Mirror Tilt

Peak to Valley Wavefront Error (waves)														
	Horizontal Mirror Tilt (degrees)													
Vertical Mirror Tilt (degrees)		0	1	2	3	4	5	6	7	8	9	10	11	12
	0	0.2	1.2	2.9	5.5	8.7	12.8	17.7	23.4	30.2	35.7	44.0	53.4	64.0
	1	1.2	1.3	3.4	5.4	8.8	12.9	18.0	23.6	30.0	36.6	44.8	54.2	64.2
	2	2.9	3.0	4.9	7.2	10.4	13.9	18.9	25.0	31.3	38.4	45.7	54.7	64.7
	3	5.5	5.4	6.0	9.5	12.7	16.7	21.4	27.0	33.9	40.7	48.1	56.5	66.4
	4	8.7	8.8	9.0	12.7	14.5	19.8	24.4	29.8	36.5	44.1	52.2	59.2	68.8
	5	12.8	12.9	13.0	16.7	19.8	23.6	28.6	32.9	39.9	47.9	55.4	62.9	72.3
	6	17.7	17.9	17.8	21.4	24.4	28.2	33.0	38.9	43.5	51.7	60.8	67.9	76.7

mirror location. This is done to characterize the on-axis system and determine if the proper resolution requirements have been met. The primary mirror is attached to a gimbal mount designed to keep the optical surface centered at the axis of rotation for both horizontal and vertical mirror tilt.

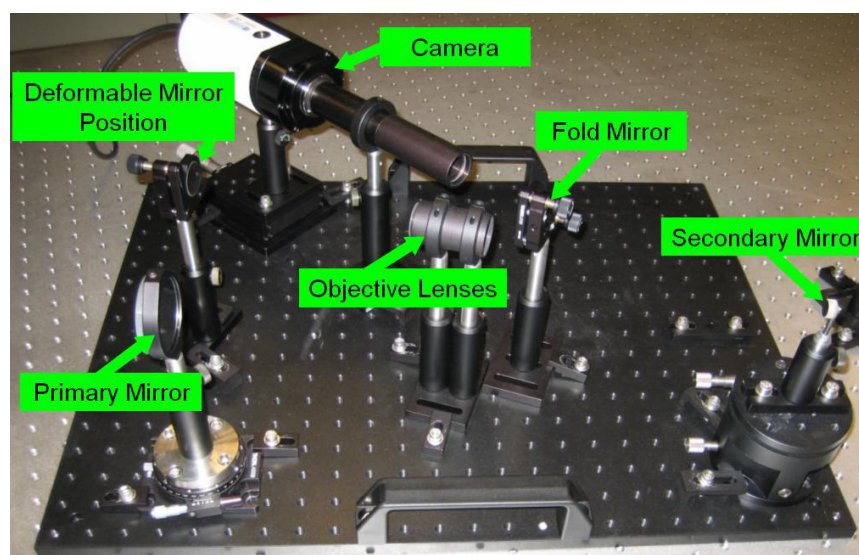


Figure 1. Experimental Telescope Setup Without Deformable Mirror

A USAF 1951 optical calibration target printed on 8.5x11 inch paper is placed outside at a distance of 250 meters from the telescope to verify the system's performance. It is immediately evident that atmospheric disturbances are present and these cause difficulty in obtaining an image that can be used to reliably determine the telescope's resolution. Each image that is captured produces different resolution limits so a series of shots are taken and some of the better images are used. A resolution of 5mm/line pair is achieved with this setup.

Based on the size of the primary aperture of the telescope, the resolution is calculated to be 4.4 mm/line pair. The difference in the measurement of 5 mm/line pair and the calculated value of 4.4 mm/line pair is not too surprising due to the atmospheric disturbances and less than ideal lighting conditions. We determined that it would not be fully possible to test the telescope and deformable mirror in these outdoor conditions. A comparable setup must be tested in a controlled environment where the effects of off-axis scanning can be determined.

4. LABORATORY TESTING AND OPTIMIZATION

An equivalent telescopic system is built on an optical table indoors. In order to compensate for the reduced target distance, a positive lens with a 600mm focal length is placed in front of the telescope and an illuminated USAF 1951 optical calibration target is placed at the focal plane of the lens. This setup collimates the incoming

light creating the illusion that the target is equivalently at a great distance. During testing, it is necessary that the distance from the primary mirror to the positive lens and from the lens to the target be the same no matter what angle the primary mirror is at. To accomplish this, the telescope assembled on the breadboard is allowed to pivot about the axis of the primary mirror while attached to the optical table. The mirror can pivot on the same axis to point at the target and acquire the test images.

As the primary mirror is scanned to off-axis angles, there is obvious degradation in the image quality due to the aberrations introduced into the system. In order to quantify the level of image degradation, a "sharpness" metric is used. This calculation of sharpness, S is given as:

$$S = \sum_x \sum_y I^2(x, y), \quad (1)$$

where x is the pixel row, y is the pixel column, and I is the normalized pixel intensity value.⁹ For this metric, a higher value represents a sharper image.

While there is not an exact correlation between the sharpness calculation and the MTF, they are both a measure of the quality of the image. Figure 2 (left) is a plot of the image sharpness values recorded at 1-degree increments for field angles between -5 and 5 degrees. This curve is comparable to the plot on the right which shows ZEMAX simulation results for MTF vs. field angle for various obscuration sizes. In particular it matches well to simulations with larger obscurations. It is clear by the experimental data that there is image degradation over field angles when the obscuration is in the way. The fact that there is slightly more degradation in the laboratory setup is consistent with the resolution seen in outdoor experiments.

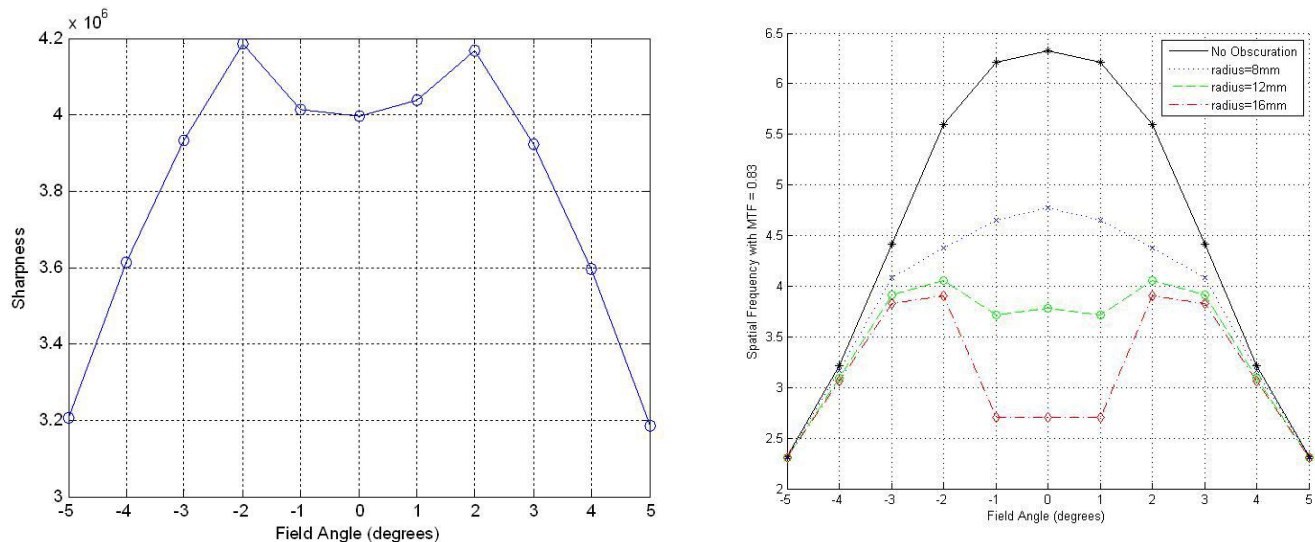


Figure 2. Sharpness vs. Field Position at 1-Degree Increments for Experimental Results (left) and ZEMAX Simulations with Various Obscuration Effects (right)

Because the off-axis aberrations introduced into the system are field angle dependent, they can be characterized and compensated for with a deformable mirror as the field angle changes while scanning. Even though ZEMAX simulations can determine a mirror surface required to remove the aberrations, simply telling the deformable mirror to match that same surface profile is not easily accomplished. Each actuator is controlled by an input voltage, but the stroke of the actuator is not linearly proportional to the magnitude of the applied voltage. Actuators are affected by neighboring actuator sites and as the voltage changes in a single site, the surface profile over a group of actuators is affected. Different deformable mirrors also have varying rigidity in the mirror surface materials which adds to the complexity of developing a model that will work for any single system.

For this design, the deformable mirror surface profile is determined by optimizing the applied actuator voltages relative to the sharpness of the image calculated from Eq. 1. The optimization is a gradient ascent method that looks for a maximum value corresponding to the sharpness of the image. This process is derived from a similar method used to calibrate the ASOM.¹⁰ The algorithm is as follows:

- A perturbation is applied to each actuator individually in the form of a positive and negative voltage step.
- An image is taken after each perturbation and the sharpness is calculated.
- Based on the best sharpness value obtained over all actuators, a line search is performed at the actuator site of the best sharpness value and the highest value of that search is saved.
- The actuator voltages are then updated to reflect the new voltage at the actuator.
- This process is repeated until the optimal resolution of the system is achieved or until the actuators saturate at their stroke limits.

After the mirror is optimized at a field position, a new field position is chosen and the entire optimization begins again. The optimized actuator voltages at incremental field positions are stored so that they can be recalled to set the shape of the mirror surface at the appropriate location when scanning. It is not practical to optimize the mirror surface at every field location so interpolation can be used for field positions between those actually optimized for.¹⁰

5. OPTIMIZATION AND TEST RESULTS FOR AGILOPTICS MIRROR

Two different deformable mirrors are tested in the telescope setup. The first is a 61-actuator, $6\mu\text{m}$ stroke mirror manufactured by AgilOptics. Input voltages on this mirror range from 0 to 160 volts. Actuators on this mirror can only pull the mirror surface down so it is necessary to bias the input voltages at 80 volts in order to set the mirror near the center of its dynamic range. This way the actuators can "push up" by lowering the applied voltage.

Once the bias is set, the telescope is aligned and focused on axis. Images are acquired with a QImaging Retiga 2000R cooled monochromatic camera with a 1600×1200 resolution setting. The mirror surface optimization scheme is performed at field positions every two degrees. A two degree rotation of the telescope results in a one degree tilt of the primary mirror.

Optimizations are allowed to run until the desired resolution is met or until the actuator voltages reach their limits and further correction is no longer possible. Figures 3 and 4 show the corrected images at 5 and 6 degree mirror tilt, respectively. Accompanying each image is a plot of the intensity of the bar pattern associated with the resolution limit of the image. The dashed line indicates 74% of the maximum intensity in the pattern which is the limit where two separate lines are just resolvable if the trough between them is below the line. The solid line represents the maximum intensity of the pattern.

For 5-degree tilt in Figure 3, the smallest resolvable bar pattern is Group 6 Pattern 4. In Figure 4 the smallest resolvable bar pattern at 6-degree tilt is Group 6 Pattern 3. At this point the image has not only decreased in resolution but many of the actuators have reached their voltage limits and can provide no further correction. Upon first seeing these results, it seems as if the mirror is not performing to the full extent it is capable of. With a stroke of $6\mu\text{m}$, the mirror should be able to correct for 21.8 waves of aberration (based on a 550nm wavelength) and, according to Table 1, 6-degrees of tilt results in only 17.7 waves of aberration. At this point we need to consider that with an aberration such as astigmatism, only a fraction of the full stroke can be realized due to a more complex surface shape.

Specifications on the performance of the mirror's surface while set to various common aberration profiles are not listed in AgilOptics user's manual so the actual reduction in full stroke while compensating for astigmatism is not known. It is clear from the resolution data that there is a degradation in performance after 5-degrees of mirror tilt which corresponds to 12.8 waves of aberration or 59% of the full mirror stroke. A 6-degree tilt corresponds to 17.7 waves of aberration or 81% of the full mirror stroke.

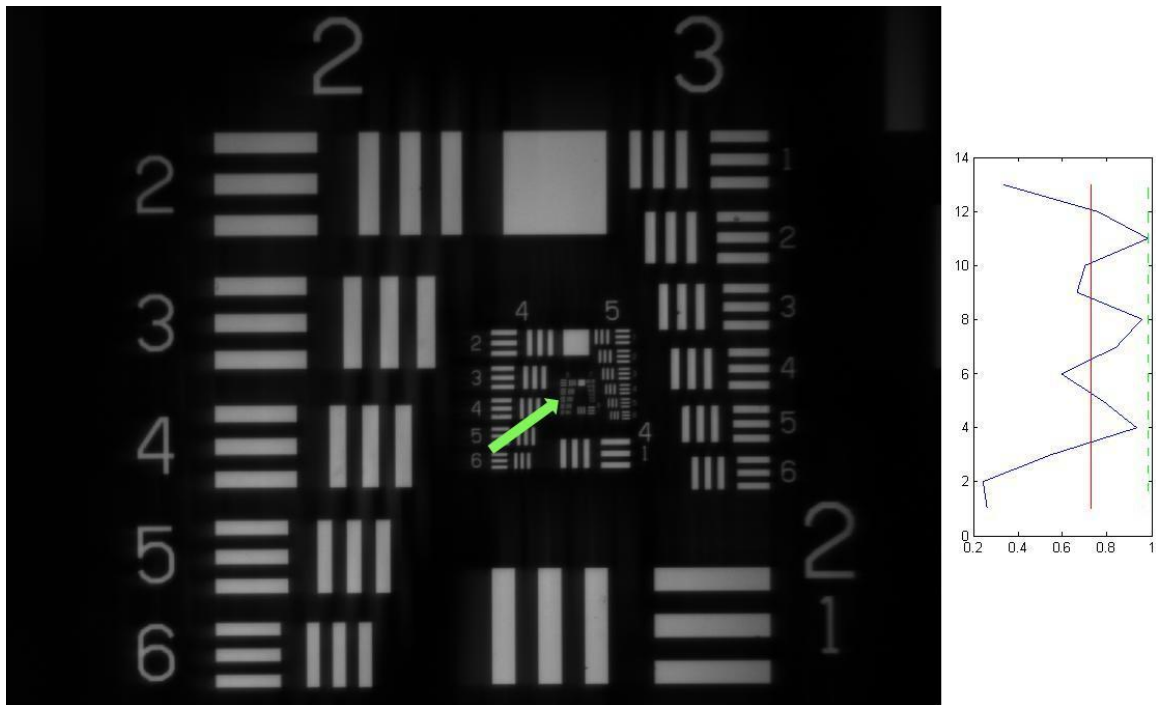


Figure 3. AgilOptics: Corrected Image with Mirror Tilt=5 degrees

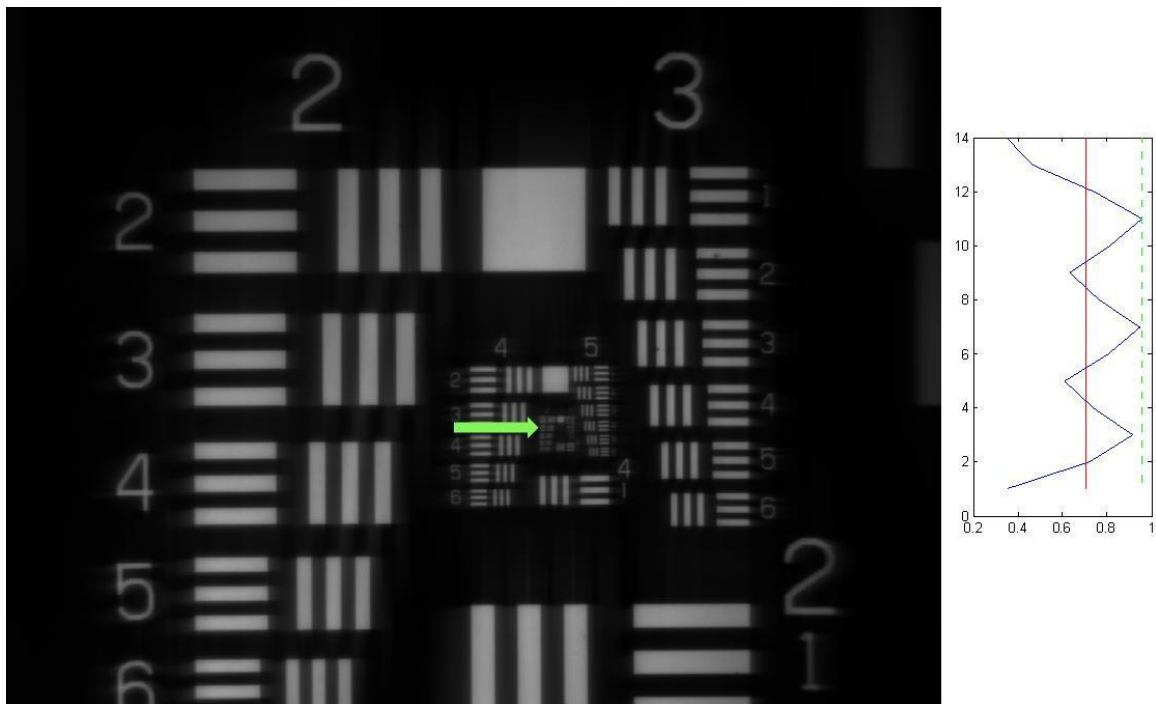


Figure 4. AgilOptics: Corrected Image with Mirror Tilt=6 degrees

With a mirror tilt of ± 5 -degrees, a field angle of 10-degrees can be acquired in two directions resulting in a 20-degree horizontal field of view. This overall horizontal field of view is 40.8 times larger than an equivalent stationary telescope with the same resolution. If the experiments are expanded to allow vertical mirror tilt, according to the simulation results in Table 1, the expected rectangular field of view maintaining the same

4:3 aspect ratio would be 16-degrees horizontally and 12-degrees vertically. This corresponds to horizontal and vertical fields that are 32.7 times as large as the original field size or a field area that covers 1064 times the area of an equivalent stationary telescope.

6. OPTIMIZATION AND TEST RESULTS FOR MIRAO-52D MIRROR

The same optimization technique is used on a second deformable mirror from Imagine Eyes. The Mirao-52d, has 52 actuators capable of $\pm 50\mu\text{m}$ stroke.¹¹ The applied voltage range is between $\pm 1\text{V}$. Figure 5 shows the resolution limit of the Mirao on-axis to be at Group 6 Pattern 3 which is less than the resolution obtained by the AgilOptics mirror. The reduced image resolution is possibly due to fewer actuators (52 versus 61) to obtain an ideal mirror surface. For on-axis imaging, there is still some higher order wavefront aberration produced by the lens elements. The closer the spacing of the actuators, the finer the correction, and it is clear that the reduction in actuators results in lower image resolution.

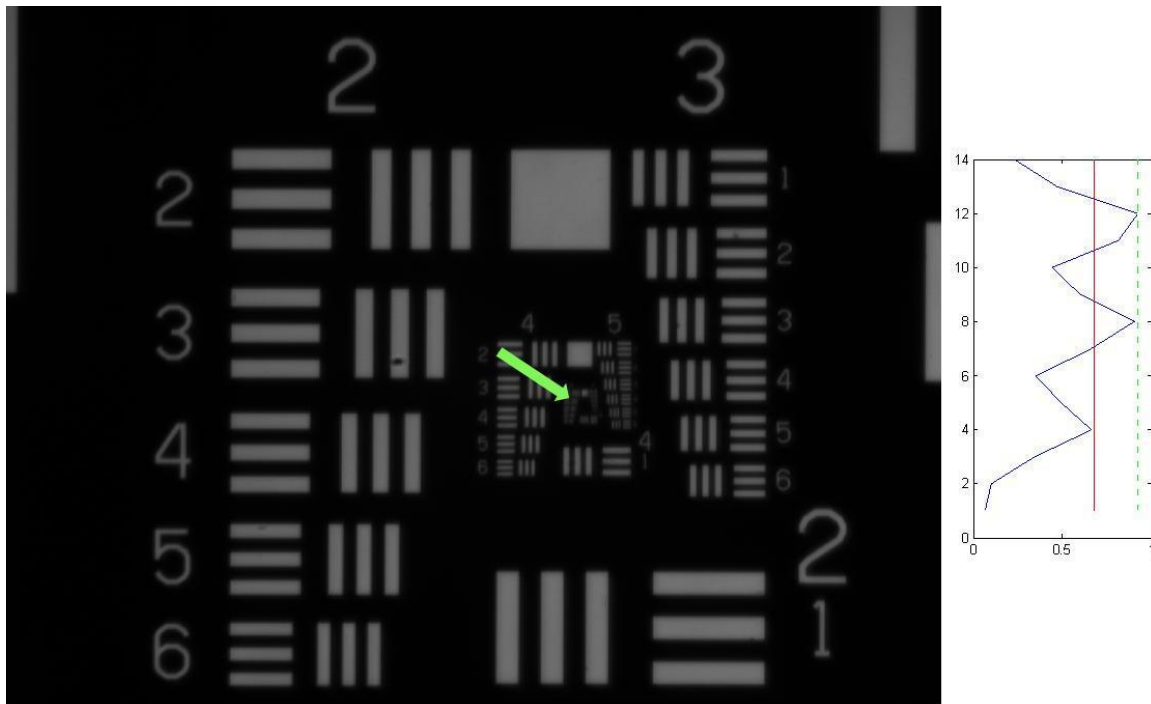


Figure 5. On-Axis Target with Mirao-52d

For a mirror tilt of 10-degrees in Figure 6 the mirror is still able to meet the resolution limit for the same bar pattern. At an angle of 11-degrees, the resolution limit drops to Group 6 Pattern 2. These results are also consistent with ZEMAX simulations. In Table 1, 10-degrees of horizontal tilt produces 44 waves of aberration, or equivalently $24\mu\text{m}$ of actuator stroke is necessary for correction. According to documentation by Imagine Eyes, the maximum peak to valley correction for astigmatism is $30\mu\text{m}$.¹² The Mirao has issues with the actuator coils overheating if they are kept on too long at greater than 0.5 volts, so limits have been set at 0.4 volts. This essentially reduces the stroke to 40% of the maximum. 40% of $30\mu\text{m}$ is $12\mu\text{m}$ of stroke that produces $24\mu\text{m}$ of peak to valley correction and we show that this correction is met. An angle of 11-degree tilt corresponds to 53.4 waves ($29\mu\text{m}$) of correction but the maximum is $24\mu\text{m}$ and this is why we see the reduction in image resolution at 11-degree tilt.

An attempt is made to increase the achievable stroke by adjusting the voltage limits to 0.5 volts but the Mirao's amplifier goes into protection mode during the optimization. A mirror tilt of 10-degrees is the maximum that can be corrected for with this mirror with the voltage limitations. From Figure 7, it is clear that the image corrected with the Mirao at 10-degrees (right) is a significant improvement to the uncorrected image (left).

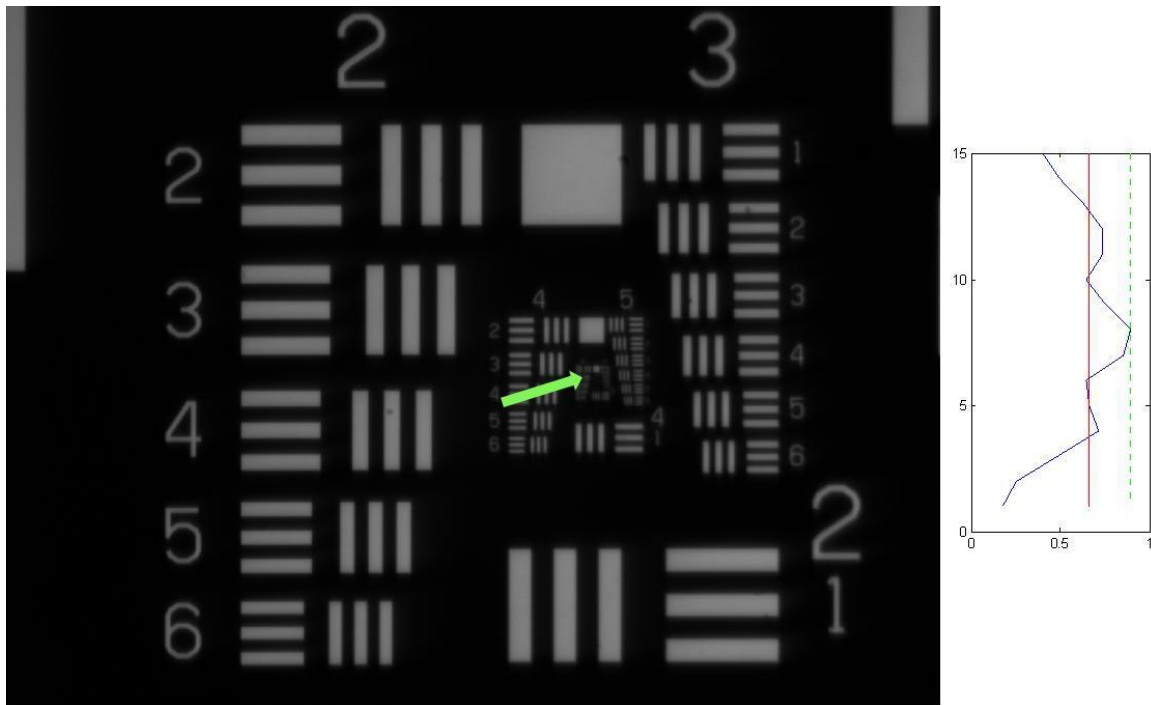


Figure 6. Mirao: Corrected Image with Mirror Tilt=10 degrees

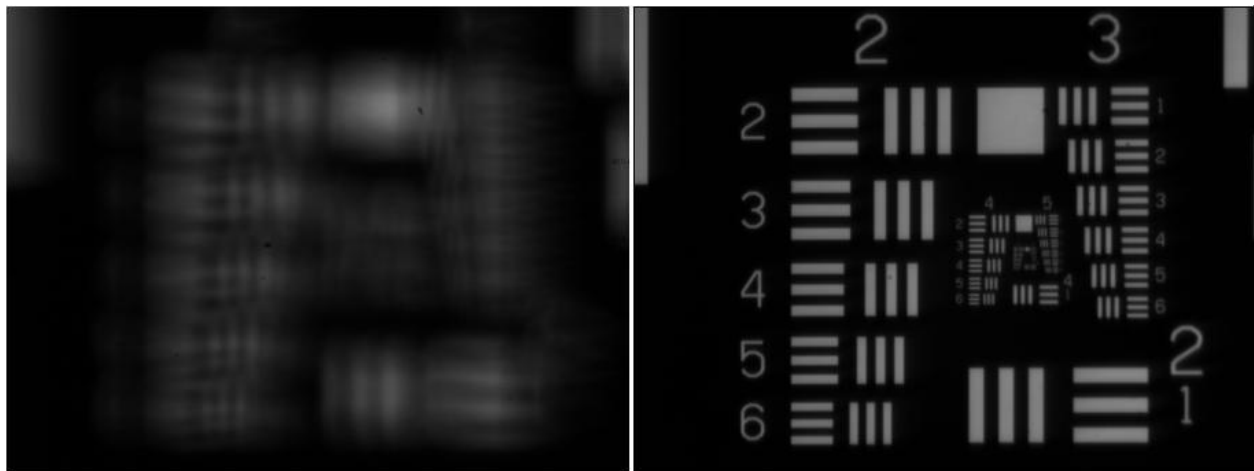


Figure 7. Uncorrected Image, Tilt=10-degrees (left), Corrected Image, Tilt=10-degrees (right)

For the Mirao, a full ± 10 -degrees of horizontal mirror tilt is obtained while maintaining the same resolution as on-axis. This results in a horizontal field angle of 40-degrees which is just over 80 times larger than a stationary telescope with the same resolution. If this experimental setup were modified for vertical mirror tilt, simulation results from Table 1 indicate that it is possible to expand the rectangular field of view with a 4:3 aspect ratio to 36-degrees horizontally and 24-degrees vertically. This results in a field area that is 4,264 times larger than an equivalent stationary telescope. If actuator overheating is not an issue and the full stroke of the mirror can be achieved, 109 waves of aberration can be corrected for instead of 44 waves.

7. SUMMARY AND FUTURE WORK

We have shown both by simulation and experimental methods that it is possible to increase the field of view in a telescope by scanning the primary mirror and correcting for the aberrations introduced with deformable mirror

technology. While this method differs from traditional telescope design, it provides a viable option to obtain a wide field of view at high resolution. A summary of the experimental results comparing both mirrors tested is found in Figure 2. Limitations as to the maximum obtainable field of view are subject to the performance of the deformable mirror in its ability to remove aberrations. Our simulated results match the experimental performance of the two deformable mirrors that were tested. With the AgilOptics deformable mirror, the field of view can be increased to 40.8 times its original size. With the large stroke of the Imagine Eyes mirror, the field of view can be increased to 81.6 times its original size while maintaining high resolution.

Table 2. Summary of Experimental Results

	Deformable Mirror Type	
	AgilOptics	Mirao
Maximum Actuator Stroke	6 microns	50 microns (20 microns in practice)
Percentage of Full Actuator Stroke Used	58.30%	60% (of 20 microns)
Maximum Peak-to-Valley Astigmatism Correction	7microns, 12.8 waves	24 microns, 44 waves
Maximum Correctable Mirror Tilt	5 degrees	10 degrees
Maximum Correctable Field of View	20 degrees	40 degrees
Increase From Single Field Size	40.8 times	81.6 times

It is clear by both simulations and experimental results that a larger field of view can be acquired provided that the aberrations due to scanning can be compensated for. Additionally we see that the aberrations increase proportional to the square of the field angle therefore it becomes increasingly difficult to remove these aberrations at larger angles. The current design discussed in this paper was created such that on-axis imaging is diffraction limited but off-axis image quality quickly degrades. Future designs can incorporate a different static optics design that removes more aberrations off-axis while sacrificing optical quality on-axis. This approach is used by the ASOM and relies on the deformable mirror to correct for aberrations both on and off-axis.⁸ The advantage to this type of design is that the magnitude of off-axis aberrations can be reduced resulting in larger scanning angles.

For our current system, the optimization of the deformable mirror at a given field position can take anywhere from an hour to half a day to complete. This is due largely to the use of the MATLAB optimization toolbox and the communication delay between MATLAB and the camera. We anticipate a significant reduction of the optimization time once this architecture is improved. Once the mirror optimization time is reduced, it is advantageous to perform the optimization on as many discrete field positions as possible for better system performance. More research can be put into creating a better model for the deformable mirror surface so ZEMAX can be used to accurately simulate the mirror and corresponding actuator voltages. In order to create this model, the actual surface of the mirror will have to be accurately measured as the voltages are changed and this information can be compared to the theoretical surface. Surface optimizations would no longer be necessary and control voltages could be directly calculated for any field position using ZEMAX simulations and the actual surface model.

Acknowledgment

This work is also supported in part by the Center for Automation Technologies and Systems (CATS) under a block grant from the New York State Foundation for Science, Technology and Innovation (NYSTAR). The authors would also like to thank Imagine Optics, Inc., for providing a demonstration Mirao 52-d deformable mirror for testing, and Thorlabs, Inc., for providing various optical components used in this work. John Wen is supported in part by the Outstanding Overseas Chinese Scholars Fund of Chinese Academy of Sciences (No. 2005-1-11).

REFERENCES

- [1] Fischer, R. E. and Tadic-Galeb, B., [*Optical System Design*], McGraw-Hill, New York (2000).

- [2] Guestrin, C., Cozman, F., and Godoy Simoes, M., "Industrial applications of image mosaicing and stabilization," *Knowledge-Based Intelligent Electronic Systems, 1998. Proceedings KES '98. 1998 Second International Conference on* **2**, 174–183 vol.2 (21-23 Apr 1998).
- [3] Peter A. Jansson, Wade T. Rogers, J. S. S., "Electronic mosaic imaging process." United States Patent 4,673,988 (1987).
- [4] Gruneisen, M. T., Garvin, M. B., Dymale, R. C., and Rotge, J. R., "Agile-field telescope system with diffractive wavefront control," in [*Advanced Wavefront Control: Methods, Devices, and Applications III. Edited by Gruneisen, Mark T.; Gonglewski, John D.; Giles, Michael K. Proceedings of the SPIE, Volume 5894, pp. 345-350 (2005).*], Gruneisen, M. T., Gonglewski, J. D., and Giles, M. K., eds., *Presented at the Society of Photo-Optical Instrumentation Engineers (SPIE) Conference* **5894**, 345–350 (Aug. 2005).
- [5] Wick, D., Martinez, T., Restaino, S., and Stone, B., "Foveated imaging demonstration," *Opt. Express* **10**(1), 60–65 (2002).
- [6] Martinez, T., Wick, D., and Restaino, S., "Foveated, wide field-of-view imaging system using a liquid crystal spatial light modulator," *Opt. Express* **8**(10), 555–560 (2001).
- [7] Bifano, T. G., Perreault, J., Mali, R. K., and Horenstein, M. N., "Microelectromechanical deformable mirrors," *IEEE J. Sel. Top. Quantum Electron.* **5**, 83–90 (1999).
- [8] Potsaid, B., Bellouard, Y., and Wen, J., "Adaptive scanning optical microscope (ASOM): A multidisciplinary optical microscope design for large field of view and high resolution imaging," *Opt. Express* **13**(17), 6504–6518 (2005).
- [9] Muller, R. A. and Buffington, A., "Real-time correction of atmospherically degraded telescope images through image sharpening," *J. Opt. Soc. Am.* **64**(9), 1200 (1974).
- [10] Potsaid, B., Rivera, L. I., and Wen, J. T.-Y., "Adaptive scanning optical microscope (ASOM): large field of view and high resolution imaging using a MEMS deformable mirror," in [*MEMS Adaptive Optics. Edited by Olivier, Scot S.; Bifano, Thomas G.; Kubby, Joel A.. Proceedings of the SPIE, Volume 6467, pp. 646706 (2007).*], *Presented at the Society of Photo-Optical Instrumentation Engineers (SPIE) Conference* **6467** (Mar. 2007).
- [11] "Mirao52d deformable mirror user's guide," (2006).
- [12] "http://www.imagine-optic.com/," (2007).